

# High precision measurement of the differential $W$ and $Z$ boson production cross sections with the ATLAS experiment

---

**Philip Sommer on behalf of the ATLAS collaboration**

*Albert-Ludwigs-Universität Freiburg*

*E-mail:* [philip.sommer@cern.ch](mailto:philip.sommer@cern.ch)

Measurements of the Drell–Yan production of  $W$  and  $Z/\gamma^*$  bosons at the LHC provide a benchmark of our understanding of perturbative QCD and probe the proton structure in a unique way. The ATLAS collaboration has performed new high precision measurements at centre-of-mass energies of 7 TeV. The measurements are performed for  $W^+$ ,  $W^-$  and  $Z/\gamma^*$  bosons integrated and differentially as a function of the boson or lepton rapidity and the  $Z/\gamma^*$  mass. Unprecedented precision is reached and strong constraints on parton distribution functions, in particular the strange quark density, are derived.

*XXV International Workshop on Deep-Inelastic Scattering and Related Subjects*

*3-7 April 2017*

*University of Birmingham, UK*

## 1. Introduction

Measurements of the Drell–Yan production of vector bosons which subsequently decay leptonically are amongst the most precise measurements at hadron collider experiments due to the large event rates and relatively clean experimental signatures. Recent measurements of inclusive and differential  $W^\pm \rightarrow \ell^\pm \nu^{(-)}$  and  $Z/\gamma^* \rightarrow \ell^+ \ell^-$  production cross sections have been performed on a dataset of  $4.7 \text{ fb}^{-1}$  of proton–proton collisions at a centre-of-mass energy of 7 TeV [1] recorded by the ATLAS detector [2] in the year 2011. These measurements significantly improve on previous results based on a dataset recorded in the year 2010 [3] at the same centre-of-mass energy by reducing uncertainties and increasing the granularity of differential measurements.

At the same time the Drell–Yan process is theoretically known extremely well. Calculations are available at next-to-next-to leading order in  $\alpha_S$  and next-to-leading order in  $\alpha_{EW}$ . Precise measurements of the  $W$  and  $Z$  production cross sections can be used to infer on the uncertain input to the theoretical calculations. For Drell–Yan production, theoretical uncertainties due to missing higher order corrections are roughly  $\pm 1.1\%$  while uncertainties on the parton distribution functions of the proton (PDFs) can be as large as  $\pm 2.5\%$  with a spread between different PDF sets even larger than this. In the following, the measurements are described and used to derive constraints on the proton PDFs, to test lepton universality in  $W^\pm \rightarrow \ell^\pm \nu^{(-)}$  and  $Z/\gamma^* \rightarrow \ell^+ \ell^-$  decays and to provide a direct measurement of the coupling of charm and strange quarks  $|V_{cs}|$ .

The production of  $W$  and  $Z$  bosons probe the proton structure at a momentum transfer just below  $Q^2 = 10^4 \text{ GeV}^2$ . Differential cross-section measurements as a function of the lepton rapidity in  $W^\pm \rightarrow \ell^\pm \nu^{(-)}$  decays and the  $Z/\gamma^*$  rapidity can provide information on the parametrisation of PDFs as a function of the momentum fraction  $x$ . Moreover, measurements in bins of the  $Z/\gamma^*$  mass probe slightly different values of  $Q^2$  and complement earlier measurements at lower [4] and higher [5]  $Z/\gamma^*$  mass.

## 2. Cross-Section Measurements

The  $W^\pm \rightarrow \ell^\pm \nu^{(-)}$  candidate events are selected by requiring exactly one electron or one muon reconstructed with a transverse momentum exceeding 25 GeV and a pseudorapidity less than 2.47 and 2.4 for electrons and muons, respectively. For electrons the transition region between barrel and endcap calorimeters at  $1.37 < |\eta| < 1.52$  is excluded from the measurement. A missing transverse momentum of 25 GeV induced by the neutrino is required. The reconstructed transverse mass of the lepton-neutrino system must be larger than 40 GeV. This selection yields approximately 13 million  $W^\pm \rightarrow e^\pm \nu$  and 15 million  $W^\pm \rightarrow \mu^\pm \nu$  candidate events where background processes are estimated to constitute 7.7% and 8.3% of the selected events.

Events from  $Z/\gamma^* \rightarrow \ell^+ \ell^-$  production are reconstructed by requiring exactly two electrons or two muons. The same pseudorapidity ranges as above are required for muons. For electrons the above requirements are only made for one of the electrons while the other electron can either fall into the above region or into  $2.5 < |\eta| < 4.9$ , excluding  $3.16 < |\eta| < 3.35$ . Events selected with one electron in the central and one in the forward region are further referred to as central-forward events and events with two central muons or electrons are further referred to as central-central events. A minimum transverse momentum of 20 GeV is required for both leptons. The electric

charge of the leptons is required to be opposite, except for central-forward events where no charge reconstruction is possible for the forward electron. The reconstructed invariant mass of the dilepton system is required to lie within 46 GeV and 150 GeV for central-central or within 66 GeV and 150 GeV for central-forward events. The selection described yields 1.3 million  $Z/\gamma^* \rightarrow e^+e^-$  and 1.6 million  $Z/\gamma^* \rightarrow \mu^+\mu^-$  candidate events.

Integrated fiducial cross sections are measured for the  $W^+$ ,  $W^-$  and  $Z/\gamma^*$  fiducial regions separately for final states with electrons and muons where all measurements are extrapolated to a common lepton acceptance of  $|\eta| < 2.5$ . These cross sections have an uncertainty on the determination of the integrated luminosity of  $\pm 1.8\%$  [6] which constitutes the largest source of uncertainty for each of the measurements. Other experimental systematic uncertainties are roughly  $\pm 1\%$  for each of the separate measurements of the fiducial  $W^\pm \rightarrow \ell^\pm \nu^{(-)}$  cross section and below 0.5% for the  $Z/\gamma^* \rightarrow e^+e^-$  and  $Z/\gamma^* \rightarrow \mu^+\mu^-$  cross sections. The experimental uncertainties of the fiducial  $W^\pm \rightarrow \ell^\pm \nu^{(-)}$  cross sections are driven by uncertainties on the estimation of background contributions from multijet and  $Z/\gamma^* \rightarrow \mu^+\mu^-$  production whereas uncertainties on the lepton reconstruction and identification, and the missing transverse momentum are only a subdominant source. The uncertainty on the  $Z/\gamma^* \rightarrow \ell^+\ell^-$  cross section is mostly due to uncertainties in the lepton reconstruction and identification.

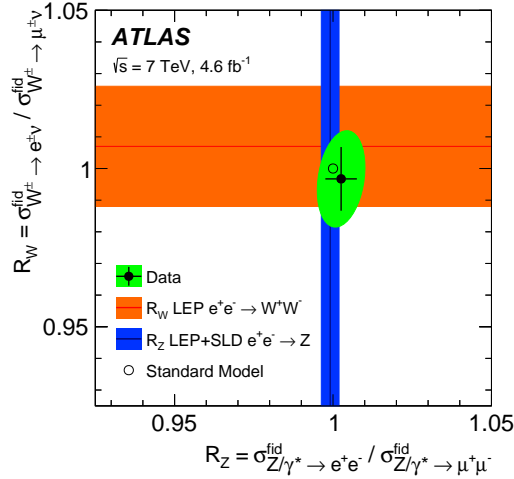


**Figure 1:** Measurement of the relative leptonic branching fractions for on-shell  $W$  and  $Z/\gamma^*$  bosons. The relative leptonic branching fractions are calculated by forming ratios of fiducial cross sections and compared to the branching fractions predicted in the Standard Model, as well as to measurements performed at LEP [1].

Ratios of the measured cross sections in electron and muon final states are formed to measure the relative leptonic  $W$  and  $Z/\gamma^*$  leptonic branching fractions,  $R_W$  and  $R_Z$ . These ratios are shown in Figure 1 and serve as a test of lepton universality. They are measured with a precision of  $\pm 1\%$  for  $W^\pm \rightarrow \ell^\pm \nu^{(-)}$  and  $\pm 0.5\%$  for  $Z/\gamma^* \rightarrow \ell^+\ell^-$  decays. Both quantities are found in agreement with the expectation in the Standard Model of  $R_W = R_Z = 1$ . The measurement of the relative  $W^\pm \rightarrow \ell^\pm \nu^{(-)}$  branching fraction is the most precise result for on-shell  $W$  bosons. The measurement improves on previous results from the LEP experiments [7], reducing the uncertainty by 50%.

Assuming lepton universality the measurements from final states with electrons and muons

can be combined. The systematic uncertainties in the lepton reconstruction and the background estimation are mostly uncorrelated between the individual measurements, resulting in even lower uncertainties on the leptonic cross sections, reaching 0.5% for  $W^+ \rightarrow \ell^+ \nu$ , 0.6% for  $W^- \rightarrow \ell^- \bar{\nu}$  and 0.3% for  $Z/\gamma^* \rightarrow \ell^+ \ell^-$  with a common additional uncertainty of  $\pm 1.8\%$  from the luminosity determination.

Differential measurements are performed with the aim of constraining PDFs. The measurement of differential  $W^\pm \rightarrow \ell^\pm \nu^{(-)}$  cross sections is using ten bins in the lepton pseudorapidity. The bin boundaries are chosen to optimally capture the cross-section shape while assuring control of local detector effects. Measurements of differential  $Z/\gamma^* \rightarrow \ell^+ \ell^-$  cross sections are performed in  $Z/\gamma^*$  mass bins of  $46 < m_{\ell\ell} < 66$  GeV (not for central-forward events),  $66 < m_{\ell\ell} < 106$  GeV and  $106 < m_{\ell\ell} < 150$  GeV. Each of these measurements is separated into twelve bins (central-central events) or nine bins (central-forward events) of the  $Z/\gamma^*$  rapidity. The measurements cover a range up to 3.6, where for values larger than 2.4 only central-forward events can be used. The use of forward electrons therefore significantly extends the reach of the measurement to higher values of the  $Z/\gamma^*$  rapidity. Differential measurements from final states with electrons and muons are combined using a  $\chi^2$  minimisation. Results from final states with electrons and muons nicely complement each other as their precision varies with pseudorapidity. Excellent agreement between electron and muon final states is found with  $\chi^2/\text{n.d.f.} = 47.2/44$ .

### 3. Comparison with Theory

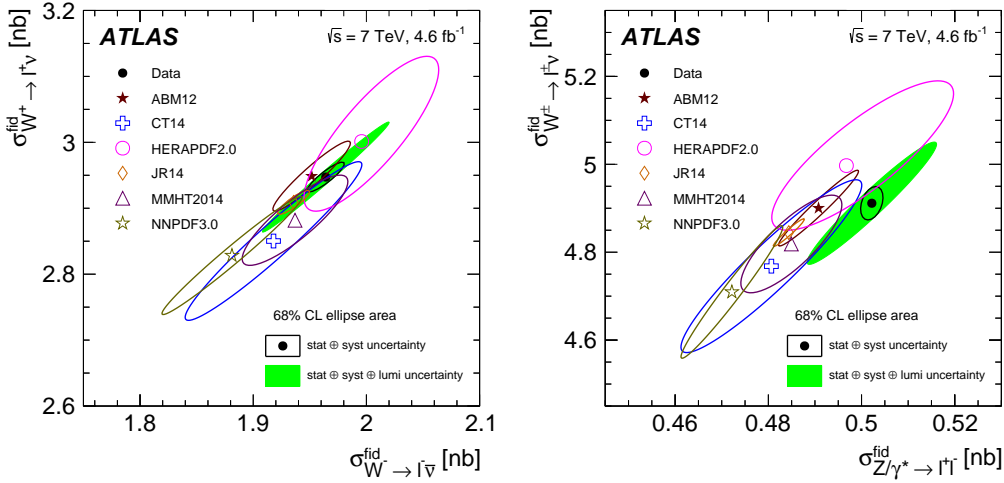


**Figure 2:** Fiducial  $W^+ \rightarrow \ell^+ \nu$  and  $W^- \rightarrow \ell^- \bar{\nu}$  (left), and  $W \rightarrow \ell \nu$  and  $Z/\gamma^* \rightarrow \ell^+ \ell^-$  cross sections (right). The measured values are compared to theoretical calculations from various PDF sets [1].

Theoretical predictions for the  $W^\pm \rightarrow \ell^\pm \nu^{(-)}$  and  $Z/\gamma^* \rightarrow \ell^+ \ell^-$  cross sections are calculated at next-to-next-to-leading order using DYNNLO [8, 9] and FEWZ [10–12]. Integrated fiducial cross sections obtained using different PDF sets are compared to their measured values in Figure 2. Both the  $W^+ \rightarrow \ell^+ \nu$  and the  $W^- \rightarrow \ell^- \bar{\nu}$  cross sections are generally well described by the theoretical calculations, although the predictions from MMHT2014 [13], CT14 [14] and NNPDF [15] are

lower than the measured values. The differences, however, do not exceed the uncertainty in the luminosity determination. The fiducial  $Z/\gamma^* \rightarrow \ell^+\ell^-$  cross section on the other hand is generally higher than the theoretical calculations. It can therefore provide valuable information for PDFs without the need of differential measurements. A strong correlation between the  $W^+ \rightarrow \ell^+\nu$  and the  $W^- \rightarrow \ell^-\bar{\nu}$  cross sections, and the  $W^\pm \rightarrow \ell^\pm\bar{\nu}$  and  $Z/\gamma^* \rightarrow \ell^+\ell^-$  cross sections is seen for both the theoretical and the measured values. The high measured  $Z/\gamma^* \rightarrow \ell^+\ell^-$  cross section also results in a measurement of the ratio of  $W^\pm \rightarrow \ell^\pm\bar{\nu}$  and  $Z/\gamma^* \rightarrow \ell^+\ell^-$  cross section which is significantly lower than the theoretical calculation since large parts of the experimental and theoretical uncertainties cancel.

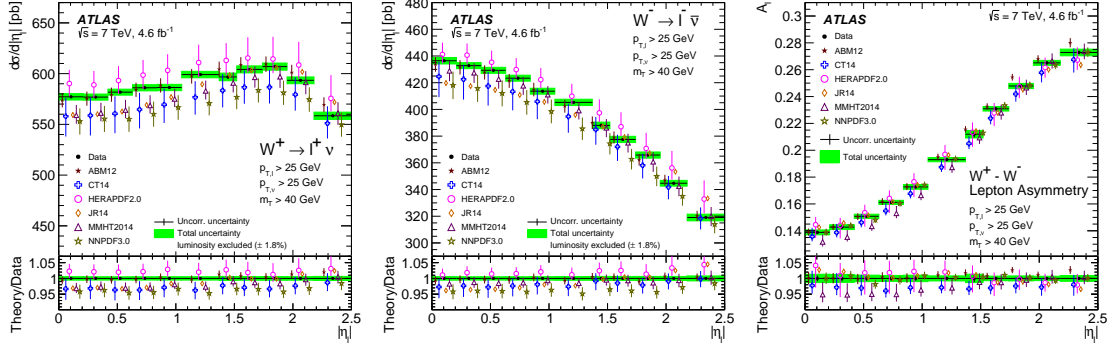


**Figure 3:** Differential measurements of the  $W^+ \rightarrow \ell^+\nu$  (left) and  $W^- \rightarrow \ell^-\bar{\nu}$  cross sections (middle), as well as the  $W^+ - W^-$  lepton asymmetry  $A_\ell$  (right). The measurements are compared to theoretical calculations from various PDF sets [1].

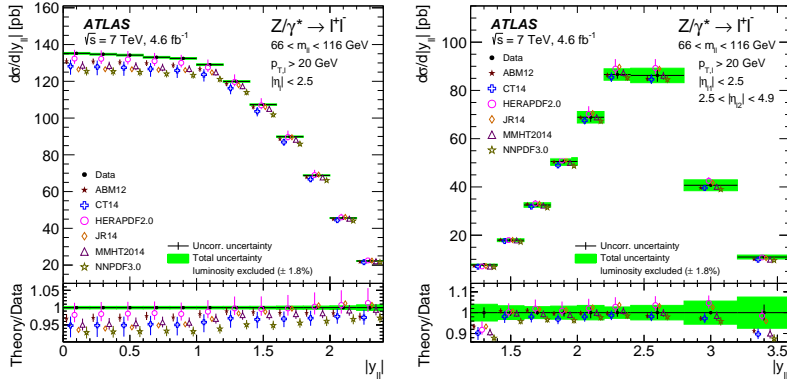


**Figure 4:** Differential measurements of the  $Z/\gamma^* \rightarrow \ell^+\ell^-$  cross sections for central-central (left) and central-forward (right) events. The measurements are compared to theoretical calculations from various PDF sets. The results are shown for a  $Z/\gamma^*$  mass of  $66 < m_{\ell\ell} < 106$  GeV [1].

A comparison of differential measurements of the  $W^+ \rightarrow \ell^+\nu$  and  $W^- \rightarrow \ell^-\bar{\nu}$  cross sections, as well as the  $W^+ - W^-$  lepton charge asymmetry  $A_\ell = \frac{\sigma_{W^+} - \sigma_{W^-}}{\sigma_{W^+} + \sigma_{W^-}}$  with theoretical predictions is shown in Figure 3. The shapes of the cross section measurements are generally well described by the theoretical calculations. A particularly good description is seen for the  $W^+ - W^-$  lepton charge asymmetry, especially when using the NNPDF3.0 PDF set which is using a similar measurement from CMS as input.

A comparison of differential measurements of the  $Z/\gamma^* \rightarrow \ell^+\ell^-$  cross sections for central-central and central-forward events with theoretical predictions is shown in Figure 4. The high measured value of the cross section is particularly distinct at central  $Z/\gamma^*$  boson rapidities and much reduced at high  $Z/\gamma^*$  boson rapidity. The measurement using central-forward events is not sensitive to differences between different PDFs.

A quantitative assessment of the agreement of the measurements with the ABM12 [16], CT14, MMHT14 and NNPDF3.0 PDF sets is achieved using a  $\chi^2$  minimisation including the measured and theoretical differential cross sections. The resulting  $\chi^2$  values are a measure of the compatibility of data with the respective PDF set. Amongst the PDFs tested, the best agreement is found with CT14 ( $\chi^2/\text{n.d.f.} = 103/61$ ) while the worst agreement is seen with NNPDF3.0 ( $\chi^2/\text{n.d.f.} = 147/61$ ). The  $\chi^2$  minimisation includes the PDF uncertainties as nuisance parameters. Their evaluation at minimum  $\chi^2$  is interpreted as the sensitivity of the PDFs to the measurements in data. The study shows that the measurements can significantly reduce the PDF uncertainties, in particular the uncertainty on the strange quark PDF. Moreover, the strange sea quark fraction is shifted to higher values. The relative strange sea fraction  $R_S = \frac{s+\bar{s}}{\bar{u}+\bar{d}}$  is shown for MMHT14 and CT14 in Figure 5 before and after the  $\chi^2$  minimisation.

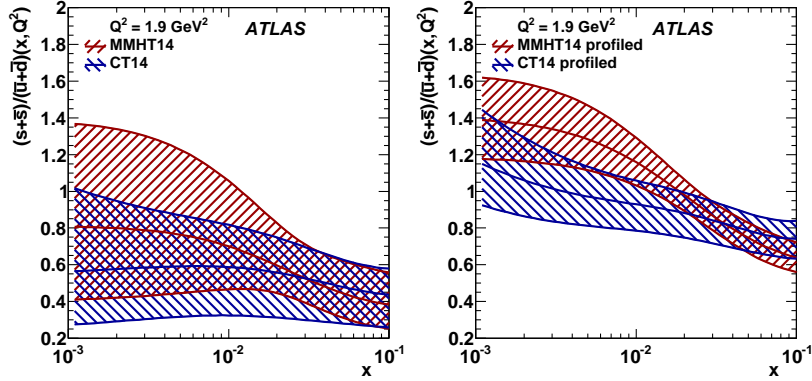


**Figure 5:** Relative strange quark sea fraction  $R_S$  for the MMHT14 and CT14 PDF sets as a function of the momentum transfer  $x$ . The distributions are shown before (left) and after (right) the  $\chi^2$  minimisation of measured and theoretical differential cross sections which includes the PDF uncertainties as nuisance parameters [1].

The differential measurements are combined with  $ep$  data from H1 and ZEUS [18] to obtain a PDF set, using the xFitter framework [17]. The ATLAS measurement adds information on the composition of the quark sea and the valence quark distributions at lower values of  $x$ . The resulting PDF set has a relative strange-to-light sea fraction of  $R_S = 1.13_{-0.08}^{+0.05}$  at  $Q_0^2 = 1.9 \text{ GeV}^2$  and  $x = 0.023$ , suggesting that the strange sea density is unsuppressed. This is in contradiction with other PDF parametrisations but in agreement with earlier results from ATLAS data [3]. Leaving the coupling of charm and strange quarks free floating in the fit provides a direct measurement of the corresponding CKM parameter  $|V_{cs}|$ , compatible with the global CKM fit and competitive with measurements from charmed meson decays.

## 4. Conclusions

The integrated and differential  $W^\pm \rightarrow \ell^\pm \bar{\nu}^{(-)}$  and  $Z/\gamma^* \rightarrow \ell^+ \ell^-$  cross sections are measured in a fiducial phase space. The measurement is performed in  $pp$  collisions at  $\sqrt{s} = 7$  TeV and significantly improves over previous measurements.

Ratios of the integrated fiducial cross sections from final states with electrons and muons serve as a test of lepton universality. The combined cross sections from final states with electrons and muons allow to discriminate between theoretical predictions obtained with various different PDF sets. A quantitative comparison of the measurement with theoretical calculations is performed and the sensitivity of the measurement to the proton structure is assessed by profiling the PDF uncertainties.

Finally, the data is combined with  $ep$  data from H1 and ZEUS and a new PDF set is obtained. The ATLAS data adds information on the flavour composition of the quark-sea and the valence-quark distributions at lower  $x$ . It is found that the strange quark sea is unsuppressed. The fit also allows for an independent direct measurement of the  $|V_{cs}|$  CKM matrix element, competitive with other measurements from charm meson decays.

## References

- [1] ATLAS Collaboration, *Eur. Phys. J. C* **77** (2017) 367.
- [2] ATLAS Collaboration, *JINST* **3** (2008) S08003.
- [3] ATLAS Collaboration, *Phys. Rev. D* **85** (2012) 072004.
- [4] ATLAS Collaboration, *JHEP* **06** (2014) 112.
- [5] ATLAS Collaboration, *Phys. Lett. B* **725** (2013) 223.
- [6] ATLAS Collaboration, *Eur. Phys. J. C* **73** (2013) 2518.
- [7] ALEPH, DELPHI, L3, OPAL and LEP Electroweak Collaborations, *Phys. Rept.* **532** (2013) 119.
- [8] S. Catani and M. Grazzini, *Phys. Rev. Lett.* **98** (2007) 222002.
- [9] S. Catani, L. Cieri, G. Ferrera, D. de Florian and M. Grazzini, *Phys. Rev. Lett.* **103** (2009) 082001.
- [10] R. Gavin, Y. Li, F. Petriello and S. Quackenbush, *Comput. Phys. Commun.* **182** (2011) 2388.
- [11] R. Gavin, Y. Li, F. Petriello and S. Quackenbush, *Comput. Phys. Commun.* **184** (2013) 208.
- [12] Y. Li and F. Petriello, *Phys. Rev. D* **86** (2012) 094034.
- [13] L. A. Harland-Lang, A. D. Martin, P. Motylinski and R. S. Thorne, *Eur. Phys. J. C* **75** (2015) 204.
- [14] S. Dulat *et al.*, *Phys. Rev. D* **93** (2016) 033006.
- [15] NNPDF Collaboration, *JHEP* **04** (2015) 040.
- [16] S. Alekhin, J. Blumlein and S. Moch, *Phys. Rev. D* **89** (2014) 054028.
- [17] S. Alekhin *et al.*, *Eur. Phys. J. C* **75** (2015) 304.
- [18] H1 and ZEUS Collaborations, *Eur. Phys. J. C* **75** (2015) 580.